Available online at www.sciencedirect.com
SCIENCE DIRECT®
Applied Geochemistry 20 (2005) 109–121
Applied Geochemistry
www.elsevier.com/locate/apgeochem

Electrochemical characterization of pyrrhotite reactivity under simulated weathering conditions

Roel Cruz [a,*], Ignacio González [b], Marcos Monroy [a]

[a] *Instituto de Metalurgia, Universidad Autónoma de San Luis Potosí, Av. Sierra Leona No. 550, Col. Lomas 2ªSección, 78210 San Luis Potosí, SLP, México*

[b] *Depto. de Química, Universidad Autónoma Metropolitana–Iztapalapa, Apdo. Postal 55-534, 09340 México DF, México*

Received 13 June 2003; accepted 25 July 2004
Editorial handling by R. Fuge

Abstract

A previously reported methodology applied to evaluate the factors affecting the reactivity pyrite and pyritic samples under simulated weathering conditions is now utilized to analyze pyrrhotite reactivity at different environmental alteration stages. The methodology is based on the comparison of the voltammetric responses of the mineral obtained through the alteration process; changes in the electrochemical behavior are associated with changes in the surface state of the mineral and finally are related with changes of the mineral reactivity. The results of an initial study of the electrochemical behavior of pyrrothite before alteration suggest that its alteration involves the formation of 3 surface layers (in agreement with previous reports): (1) in immediate contact with pyrrhotite corresponding to a metal-deficient sulfide; (2) an intermediate layer corresponding to elemental S, and; (3) the most external layer, consisting of precipitates of Fe oxy-hydroxides, like goethite. The pyrrhotite reactivity seems to be controlled by the formation of oxidation product layers that coat and passivate the pyrrhotite surface, where the elemental S layer has most significance. The results confirm the advantage of incorporating cyclic voltammetry as an auxiliary method for acid rock drainage prediction, due to its demonstrated capacity to describe the factors that influence sulfide mineral reactivity which are not evaluated by other predictive techniques.

1. Introduction

Pyrite (FeS_2) and pyrrhotite ($Fe_{1-x}S$) are the most common and abundant sulfide minerals present in mining wastes from the processing of base-metals or precious metal ores. Under environmental conditions, Fe sulfide oxidation can result in the generation of acid rock drainage (ARD). Several studies have been concerned with the oxidation mechanism of pyrite and pyrrhotite, and the chemical and structural factors affecting the dissolution of these minerals (Hamilton and Woods, 1981; Steger, 1982; Doyle and Mirza, 1990; Nicholson et al., 1990; Evangelou, 1995; Laajalehto et al., 1997; Janzen et al., 2000). In addition, many studies have been reported about the surface alteration of pyrite and pyrrhotite under acidic conditions and when these minerals are exposed to moist or dry air (Buckley and Woods, 1985a,b; Buckley et al., 1988; Sasaki, 1994; Nesbitt

* Corresponding author. Tel.: +52 44 48 25 43 26; fax: +52 44 48 25 45 84.
E-mail address: rcruz@uaslp.mx (R. Cruz).

0883-2927/$ - see front matter © 2004 Elsevier Ltd. All rights reserved.
doi:10.1016/j.apgeochem.2004.07.007

and Muir, 1994; Sasaki et al., 1995; Thomas et al., 2001; Mikhlin et al., 2002). In these studies, a large amount of data have been obtained by application of XRD and several spectroscopic techniques (i.e., XPS, AES, FTIR, Mösbauer). The generalized mechanism for pyrite oxidation at advanced stages is via thiosulfate formation, which is later oxidized to SO_4^{2-}, while the Fe is dissolved as Fe(II) and oxidized to Fe(III) with consequent formation of Fe(III) sulfate or oxide (Lowson, 1982; Sand et al., 1999). In addition, pyrrhotite dissolution studies under differing conditions have been carried out by electrochemical and spectroscopic techniques (Buckley and Woods, 1985a; Buckley et al., 1988; Nesbitt and Muir, 1994; Thomas et al., 2001; Mikhlin et al., 2002). In most of these studies the formation of a nonstochiometric, nonequilibrium or metaestable layer ($Fe_{1-x-y}S$, subsequently referred as NL) has been proposed as a result of the preferential dissolution of Fe relative to S, such as is indicated in the following reactions:.

$$Fe_{1-x}S + 0.5yO_2 + 2yH^+ \rightarrow yFe^{2+} + yH_2O + Fe_{1-x-y}S \quad (1)$$

$$Fe_{1-x}S + 0.75yO_2 + 1.5yH_2O \rightarrow yFe(OH)_3 + Fe_{1-x-y}S \quad (2)$$

Iron precipitates have been identified as Fe oxyhydroxide covering the NL. The composition and characteristics of the NL are extremely widespread depending on the conditions under which the alteration takes place. Jambor (1994) has observed various alteration sequences for pyrrhotite in different tailing impoundments: pyrrhotite to marcasite, pyrrhotite to Fe sulfate and to Fe oxyhydroxide and pyrrhotite to S. From this observation, it was concluded that the diversity of products noted in spectroscopic studies also appears in pyrrhotite from weathered tailings. Despite the knowledge acquired by the previous studies no thorough analysis of the evolution of pyrite and pyrrhotite reactivity, which could be used in the prediction of acid rock drainage has been performed. In a previous study a methodology for the analysis of factors affecting the pyrite reactivity has been presented (Cruz et al., 2001). In this study, it was concluded that in the initial stages of the alteration, the galvanic interactions between sulfide minerals present in the pyritic samples, is the main factor affecting pyrite reactivity. However, for pyrrhotite there is no in depth study about the factors affecting its reactivity under environmental conditions. Therefore, in the present work, a similar methodology to that applied to the pyrite reactivity study, is applied to analyze the effect of pyrrhotite surface state evolution, since this seems to be the main factor affecting the reactivity of this mineral.

2. Materials and methods

2.1. Mineral

The pyrrhotite sample used in this study was obtained from the El Monte Pb–Zn–Ag skarn type deposit (Zimapan, Hgo., Mexico). The sample was received in massive fragments of pyrrhotite and reduced to a particle size below 6 mm using a laboratory jaw crusher. Pyrrhotite particles not containing inclusions of other visible minerals or oxidized surface layers were selected using stereoscopic microscopy. An agate mortar was employed to crush pyrrhotite particles that were classified per sizes using standard Tyler sieves; for this study, only the particles ranging between 105 and 150 μm were used. The crushed and classified mineral was later conserved in an inert atmosphere, in the presence of N_2, within a desiccator to avoid alteration.

2.2. Electrochemical analysis

The electrochemical analyses were carried out on pyrrhotite both unleached and after different times of leaching. These analyses were accomplished by a cyclic voltammetry technique using an inert medium with the aim of characterizing the changes in the electrochemical behavior of the mineral. An EG&G PAR 273 potentiostat coupled to a PC with the M 270 software was used to impose a sweep rate of 20 mV s^{-1} and record the voltammetric response. A 3-electrode system was used consisting of a carbon paste electrode (CPE-pyrrhotite, 50 wt%) as the working electrode, a graphite rod (AlfaÆsar, 99.999% purity) as a counter electrode and a saturated sulfate electrode (SSE) ($E = 0.615$ V/SHE, standard hydrogen electrode) as a reference electrode. All potentials in this investigation are referenced to the SSE. The CPE feasibility and the details of its preparation have been previously reported by Lazaro et al. (1995).

The electrode system was placed in a Pyrex™ glass cell containing an electrolyte solution of 0.1 M $NaNO_3$ at pH 6.5. This electrolyte does not interfere with electrochemical reactions of sulfides; it offers an excellent medium for the electrochemical reactivity characterization of Fe sulfides (Cruz et al., 2001). Even though the electrolyte was not buffered, the changes in pH were not considerable, since the voltammetric experiments were performed under microelectrolysis conditions. Nitrogen was bubbled through the solution for 45 min before starting the experiments to eliminate dissolved O_2. Afterwards, the inert atmosphere was kept in the cell throughout the course of the experiments.

All voltammograms were initiated from the open-circuit potential (OCP) of the CPE-pyrrhotite in the electrolytic solution, which was necessary to achieve reproducibility of results (Hojo and Peters, 1981). The

interval of electroactivity determined for CPE-pyrrhotite in the electrolytic solution was −1.5 to 0.8 V/SSE.

2.3. Alteration device for weathering of pyrrhotite

The alteration device and procedure were designed to promote pyrrhotite oxidation under simulated environmental conditions through a cyclic procedure which alternates leaching stages and aeration stages to generate reaction rates similar to those obtained by the humidity cell procedure (ASTM, 1996; Morin and Hutt, 1997). The device consisted of 5 cm diameter polyethylene Büchner Funnels™. Twenty grams of mineral sample were placed in each funnel. A 0.45 μm paper filter was placed at the bottom of the container to retain the sulfide particles.

The leaching procedure is cyclic. It consists of one day of leaching, followed by 3 days under environmental conditions. After this, another day of leaching was followed again by two days under environmental conditions. Each leaching cycle was carried out by adding 15 mL of leach solution to each sample container, so as to completely cover the mineral sample. The samples were left inundated with the leach solution for 3 h during each leaching cycle. Leach solution was extracted from each device by vacuum suction, re-filtered (0.45 μm) and analyzed (for pH and dissolved metals as indicated below). The leach solution was formulated to simulate rainwater: distilled water with a pH adjusted to 5.5 by the addition of purified CO_2. A calculated amount of solution was prepared immediately prior to its use. A sample of mineral was taken in each leaching device just before the leaching procedure at 1, 2, 4, 6, 8 and 10 weeks for cyclic voltammetry analysis, SEM observations and X-ray diffraction analysis.

2.4. Chemical and mineralogical characterization

The pyrrhotite sample was characterized mineralogically and chemically to determine the stoichiometric composition of the pyrrhotite and the contents of mineralogical impurities, i.e., the chemical impurities in the pyrrhotite crystal lattice as well as the mineralogically associated impurities (inclusions and intergrowths). Mineral surfaces were characterized before any alteration and after several alteration cycles. Mineralogical observations were made using a Phillips XL30 scanning electron microscope (SEM) under backscattered electron image. X-ray microanalyses were performed using an EDAX 4Dix energy dispersive X-ray spectrometer (EDS) coupled to a SEM. X-ray microanalyses were performed with 20 keV electron energy, 3–5 nA beam current and 100 s of collection time. Conventional standard ZAF correction was carried out automatically for each microanalysis. The characterization of the secondary mineral phases, formed during the pyrrhotite alteration process, was complemented by X-ray diffraction (XRD) using a Rigaku DMAX 2200 X-ray diffractometer.

The chemical analysis of the pyrrhotite involved a digest step with a mixture of HNO_3 (85%) and $HClO_4$ (15%) prior to AA analysis. The AA analyses were performed with a Perkin–Elmer 5000 Atomic Absorption Spectrometer; and for total S by inductive coupled-plasma spectrometry, using a Jarell Ash Iris 25 Spectrometer. The leachates obtained during the alteration process were analyzed for pH using a Beckman ϕ320 pH meter with a combined electrode (4 N AgCl saturated). Meanwhile, analysis of dissolved metals was carried out using the same Perkin–Elmer 5000 AA Spectrometer. The limit of detection for AA analyses is 0.1 $\mu g\, g^{-1}$for solid samples and 0.1 $mg\, L^{-1}$for solution samples.

3. Results and discussion

3.1. Chemical and mineralogical composition of pyrrhotite

Mineralogical reconstruction of the sample was performed from its chemical and mineralogical analyses. In this way, the pyrrhotite sample was determined to contain 97.9% pyrrhotite ($Fe_{1-x}S$), 0.9% sphalerite (ZnS), 0.7% galena (PbS), 0.1% arsenopyrite (FeAsS) and 0.4% of non-sulfide minerals (principally quartz SiO_2). These minerals occur as inclusions in the pyrrhotite particles. The study of the content of impurities in the pyrrhotite crystal lattice indicates that pyrrhotite crystals contain Cu (0.17%), Sb (45 ppm), Co (30 ppm) and Ni (10 ppm). The mean atomic relation Fe:S is 0.89. According to this atomic relationship, the pyrrhotite has an hexagonal structure, which was confirmed by the corresponding XRD pattern. Its low Fe causes the formation of positive charge carriers, which should favor pyrrhotite oxidation (Shuey, 1975).

3.2. Voltammetric study of pyrrhotite

Since the aim of this study is to characterize pyrrhotite reactivity as a function of changes in its surface state, an electrochemical study of fresh pyrrhotite (before alteration) was carried out in order to establish a reference for the initial surface state of the mineral (i.e., electrochemical behavior of fresh pyrrhotite). This reference analysis will be later used as a basis for comparison to evaluate the reactivity evolution of pyrrhotite during its alteration process under environmental conditions. It is important to emphasize that, the electrochemical study of pyrrhotite, here presented, does not pretend to simulate its process of natural alteration, but it is used as a tool to characterize the evolution of its surface state under oxidating conditions.

Figs. 1(a) and (b) show voltammetric responses obtained for pyrrhotite when the potential sweep is initiated in positive and negative direction, respectively. When the sweep is initiated in a positive direction, an oxidation peak (O1) starting at ~0.3 V is observed (Fig. 1(a)). This peak represents a passivation process followed by a transpassive oxidation (OT). When the sweep direction is inverted, several reduction processes

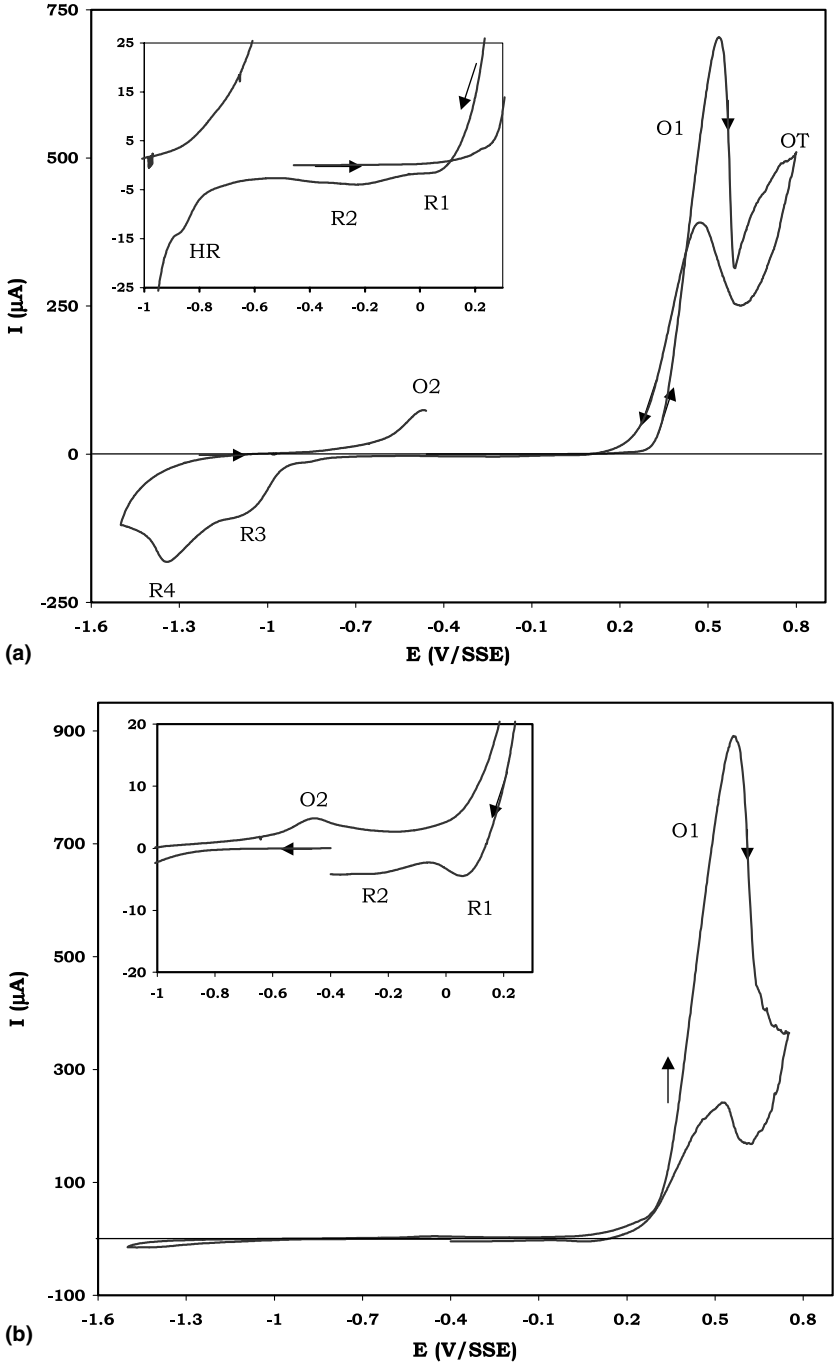

Fig. 1. Typical cyclic voltammograms of CPE-pyrrhotite in 0.1 M $NaNO_3$, when potential scan was initiated in different directions: (a) positive direction; (b) negative direction $v = 20$ mV s^{-1}. Inset figures show low-current zones of the corresponding voltammetric responses.

R1 (0.04 V), R2 (−0.2 V), HR (−0.8 V), R3 (−1.05 V) and R4 (−1.3 V) take place. Due to the low current involved in processes R1 and R2, their peaks are hardly visible in the current interval used in Fig. 1. Finally, when the potential cycle is about to be completed, a second oxidation peak (O2) appears at approximately −0.47 V (Fig. 1(a)).

When the potential sweep is initiated in a negative direction (Fig. 1(b)), a small reduction process is observed at approximately −1.3 V. When the sweep direction is inverted, a small oxidation peak similar to O2 is observed, whereas the principal oxidation peak (O1) represents different behavior from that seen when the sweep is initiated in a positive direction. It is important to point out that the reduction process, R1, is more clearly observed when the potential sweep is initiated in a negative direction.

On comparison of Figs. 1(a) and (b), it is observed that peaks R1–R4 correspond to reduction processes of species formed during the anodic scan, and that the surface of unleached pyrrhotite is free of these oxidized species. It is important to note that the initial reduction process observed during the negative direction scan potential could be associate with the reduction of pyrrhotite to stiochiometric FeS by Eq. (3) (Nicol and Scott, 1979)

$$1.12Fe_{0.89}S + 0.24H^+ + 0.24e^- \rightarrow FeS + 0.12H_2S \quad (3)$$

or to the reduction of some oxidized species performed during the handling and preparation of samples (Buckley and Woods, 1985a).

An intensive study of the voltammetric behavior of pyrrhotite was carried out by $E_{\lambda+}$ variation analysis and the data has been published elsewhere (Cruz, 2000). On the basis of this study and data reported by other authors (Hamilton and Woods, 1981; Buckley et al., 1988; Mikhlin, 2000) it can be suggested that the electrochemical oxidation process of pyrrhotite in 0.1 M $NaNO_3$, takes place in three stages, which are described as follows.

The first stage takes place at potential ranging between 0.1 and 0.25 V/SSE, which may be related to the formation of a metal-deficient sulfide, according to

$$Fe_{0.89}S \rightarrow Fe_{0.89-x}S + xFe^{2+} + 2xe^- \quad (4)$$

The reduction of this product is associated with the R4 peak at approximately −1.2 V/SSE, according to

$$Fe_{0.89-x}S + 2.24xH^+ + 2.24xe^- \rightarrow (1 - 1.12x)Fe_{0.89}S + 1.12xH_2S \quad (5)$$

The reduction process could be related to the low cathodic current observed in the voltammogram obtained when the scan is initiated in a negative direction (Fig. 1(b)).

The continuous loss of metal results in the formation of elemental S (S^0) on the mineral surface in accordance with

$$Fe_{0.89-x}S \rightarrow (0.89 - x)Fe^{2+} + S^0 + 2(0.89 - x)e^- \quad (6)$$

The amount of S^0 increases until it forms a passivating layer at potentials ~0.5 V. The $E_{\lambda+}$ analysis showed that the reduction peak R3 is associated with reduction of S, likely following the reaction

$$S^0 + 2H^+ + 2e^- \rightarrow H_2S \quad (7)$$

In a recent study Mikhlin (2000) observed the reduction of a non-stoichiometric non-equilibrium layer (NL) formed on pyrrhotite surface by HCl etching, as a lone reduction process, which involved the reduction of various S species (S_0^-, S_1^-, $(S_2)_n^{2-}$), to H_2S. The comparison of voltammograms of pyrrhotite with and without etching suggested that similar processes are involved during the electrochemical reduction of unetched pyrrhotite. However, the data shown in the current work, suggests that the reduction process of electrochemically oxidized pyrrhotite involves the reduction of S and metal-deficient sulfide in two independent processes (R3 and R4).

At potentials greater than 0.4 V, the released Fe^{2+} will oxidize according to the following reaction:

$$Fe^{2+} + 3H_2O \rightarrow Fe(OH)_3 + 3H^+ + e^- \quad (8)$$

This was demonstrated by the appearance of the reduction process characteristic of soluble Fe(III) species (peak R2). The very small size of the peak R2 is due to the fact that soluble electroactive species migrate from the interface toward the bulk solution.

Iron and S present in the electrode interface may form a Fe sulfide different from pyrrhotite, according to

$$Fe(OH)_3 + 3H^+ + e^- \rightarrow Fe^{2+} + 3H_2O \quad (9)$$

$$S^0 + Fe^{2+} + 2e^- \rightarrow FeS \quad (10)$$

The electrochemical formation of this Fe sulfide must occurs at potentials that are very close to the S^0 reduction, and could be associated to the HR process.

The last stage of the pyrrhotite electrochemical oxidation consists of the rupture of the elemental S passivating layer at potentials over 0.55 V, which occurs due to the S^0 oxidation in accordance with

$$1.12S^0 + 4H_2O \rightarrow 1.12SO_4^{2-} + 8H^+ + 6e^- \quad (11)$$

It is important to mention that the S^0 in the interface is formed again when the potential scan is reversed, as indicated by the oxidation peak appearing at potentials ~0.5 V in the oxidation process O1.

The oxidation process O2, whose peak potential is ~−0.47 V, may be related to the oxidation of H_2S formed by the reduction processes R4 and R3 (Eqs. (5) and (7)).

The data obtained in this preliminary electrochemical study of unaltered pyrrhotite will allow analysis of how the alteration of this mineral affects each electrochemical stage and these changes will be associated with changes in mineral reactivity at different times of the alteration process of pyrrhotite.

3.3. Chemical evolution of the leachate

Fig. 2 presents the chemical evolution of the leachate (pH and dissolved Fe) depending on the time of pyrrhotite alteration. During the first 3 weeks, a fast decrease in pH is observed, followed by an important instability in the pH between 3 and 6 weeks (Fig. 2(a)). After 6 weeks, the pH constantly increases until reaching a value close to 5.5 at 10 weeks of alteration. At the beginning, the Fe dissolution shows an important and constant increase until reaching a maximum value near 650 mg/L at 3.5 weeks of leaching, a period after which the concentration of Fe dissolved in the leachate constantly diminishes (Fig. 2(b)).

3.4. Electrochemical analysis of the evolution of the pyrrhotite surface state

Considering that the evolution of the pyrrhotite surface state, associated with the alteration process, must have important effects on the mineral reactivity, a voltammetric study of pyrrhotite samples was performed immediately after 1, 2, 4, 8 and 10 weeks of alteration. The objective of this study was to monitor the changes in the electrochemical behavior of pyrrhotite during its alteration process, and associate them with the reactivity evolution of the mineral sample.

Fig. 3 shows the evolution of pyrrhotite voltammetric behavior, starting in the positive-going direction, after 2, 4, 6 and 10 weeks of alteration. It can be observed that after 2 weeks of alteration (Fig. 3(b)), the oxidation process O1 decreases, while the potential, at which this process starts, displaces toward lower values. The magnitude of reduction peaks R1 and R2 increase and trend to form a single peak, as happens with R3 and R4 (R′). Since the magnitude of the current involved in the reduction processes increases in accordance with the time of leaching, it could be considered that the species formed in the electrochemical process O1 (reactions (4), (6) and (8)) are similar to those formed during the alteration process in minicells. At 4 weeks of alteration (Fig. 3(c)), important changes are observed in the pyrrhotite voltammetric behavior, the pyrrhotite oxidation process starts at lower potentials (~0.19 V) and a significant decrease in the magnitude of the current involved may be observed. In addition, a new oxidation peak (O3) is observed at −0.85 V/SSE.

As can be observed in Fig. 3(c)–(e), the pyrrhotite after 4, 6 and 10 weeks of alteration, shows very similar voltammetric behavior. However, the limited reproducibility observed for these alteration times suggests a high heterogeneity at the sample surfaces. The trend in voltammetric behavior of these samples is the decrease of the oxidation process O1 and the increase of the current involved during all reduction processes and the O2 and O3 oxidation processes.

Fig. 4 shows the evolution of voltammetric behavior, starting in negative direction, after pyrrhotite was subjected to different alteration times. Fig. 4(a)–(e) show the voltammograms obtained for unaltered pyrrhotite and after 2, 4, 6 and 10 weeks of alteration. It can be seen that after 2 weeks of alteration (Fig. 4(b)) a reduction process (R3) appears. This peak starts at approximately −1.1 V and is additional to the peak reported for unaltered pyrrhotite (at approx. −1.3 V), which at the same time increases its associated current (R4). When the scan changes direction, an oxidation peak appears at a potential similar to that of the oxidation process O2. Both the current associated with the oxidation peak O1 and the potential at which this process initiates decreases considerably. This may be associated with the appearance of another oxidation process (O4), prior to peak O1. It is worth noting the similarity between the

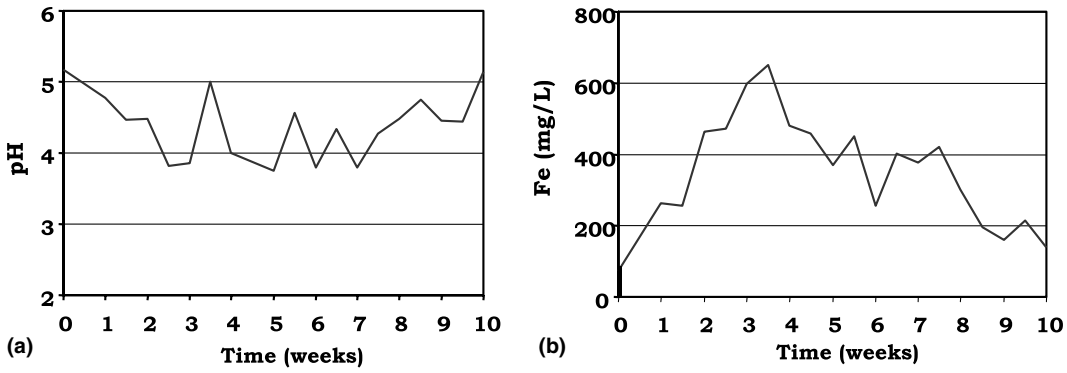

Fig. 2. Chemical evolution of leachate for: (a) pH; (b) dissolved Fe as a function of the alteration time of pyrrhotite.

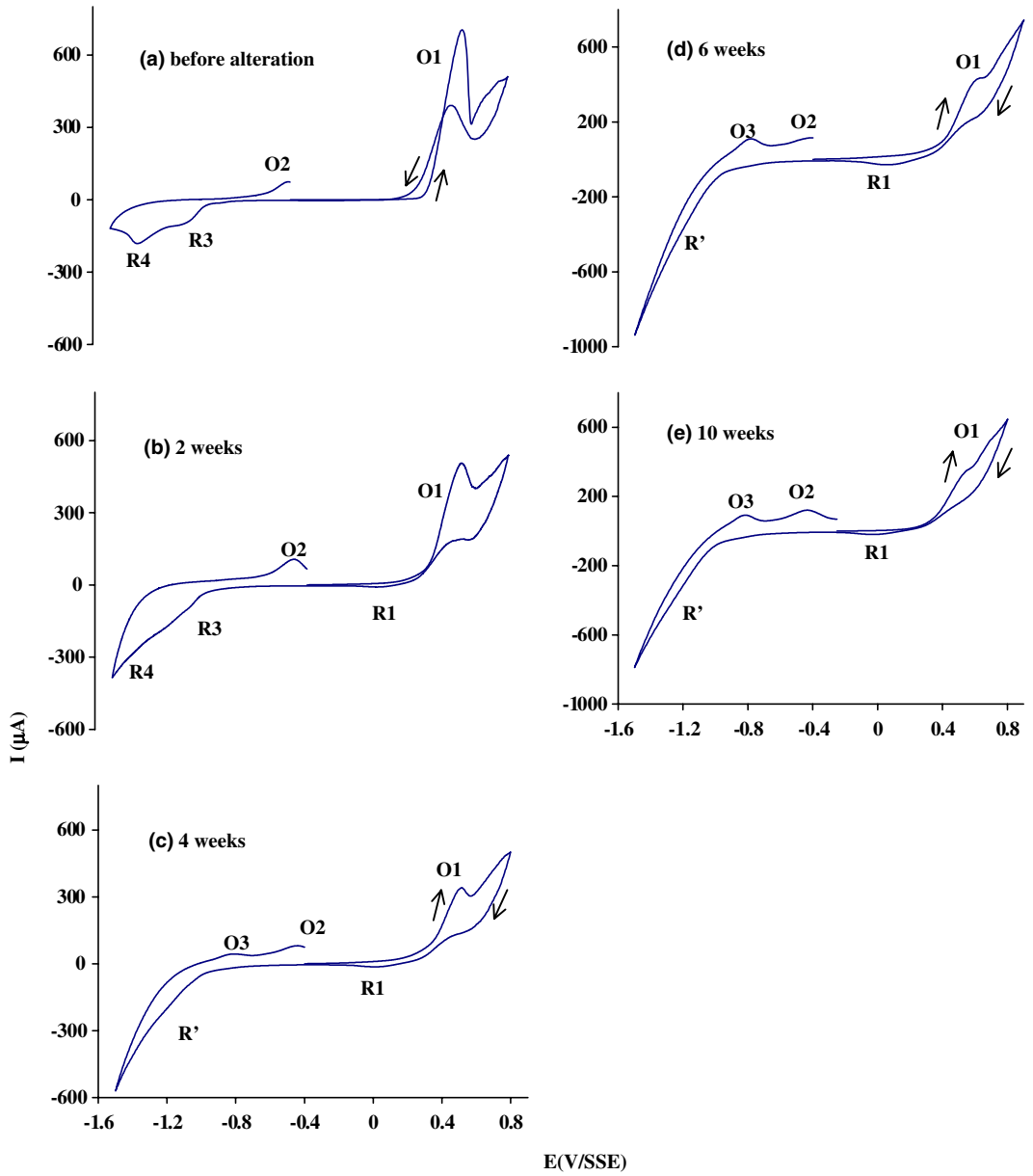

Fig. 3. Evolution of cyclic voltammetric response of CPE-pyrrhotite before alteration (a) and after several alteration times: (b) 2 weeks; (c) 4 weeks; (d) 6 weeks; (e) 10 weeks. The potential scan was initiated in positive direction, at 20 mV s^{-1}.

cathodic zones of the positive direction voltammogram of unleached pyrrhotite (Fig. 3(a)) and the negative direction voltammogram of pyrrhotite after 2 weeks of leaching (Fig. 4(b)), which could also be considered as a sign that the species formed in the electrochemical process (reactions (4), (6) and (8)) are similar to those formed during the chemical alteration process.

Corresponding to the voltammetric study initiated in the positive direction, the pyrrhotite sample shows important changes in voltammetric behavior after 4 weeks of alteration (Fig. 4(c)). The reduction processes becomes a single peak (R′) and its associated current increases significantly. In addition, an oxidation peak O3 appears at −0.85 V and the current involved in the oxidation process O4 increases provoking a decrease of the potential at which the oxidation process O1 initiates. The voltammetric responses of the pyrrhotite after 6 and 10 weeks (Figs. 4(d) and (e)) show behavior similar to that obtained for the pyrrhotite after 4 weeks of alteration.

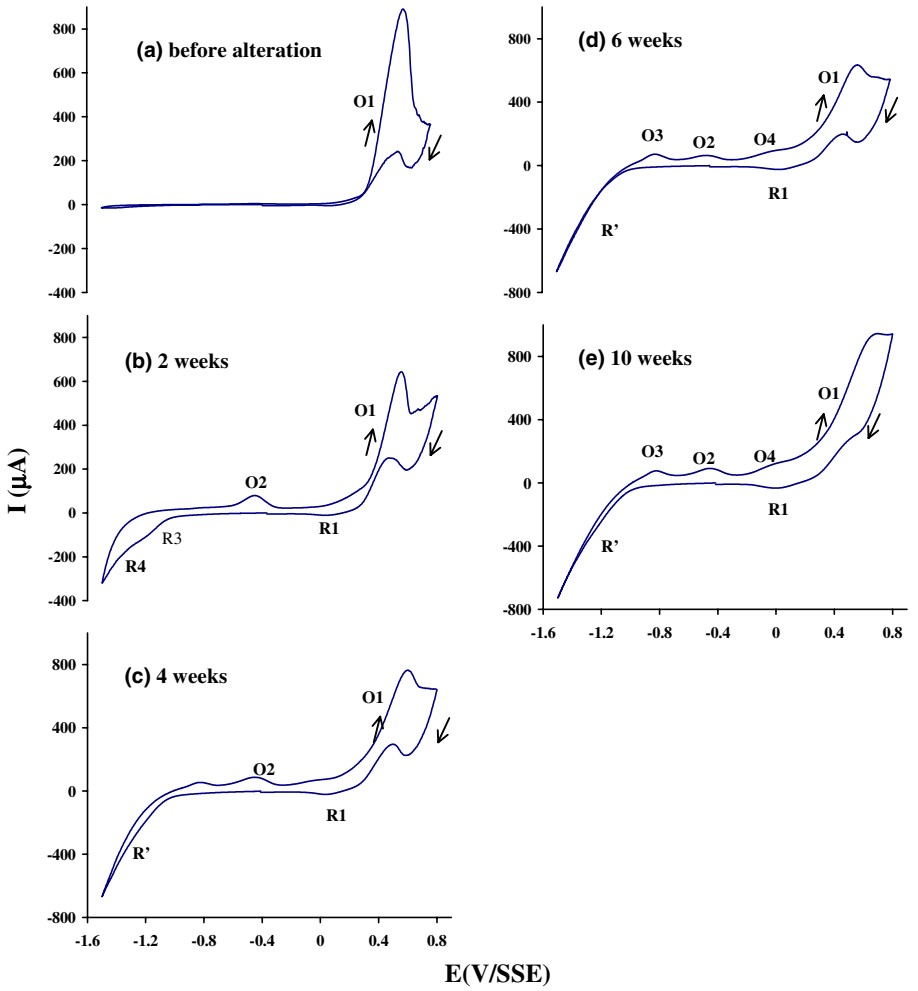

Fig. 4. Evolution of cyclic voltammetric response of CPE-pyrrhotite (a) prior to any alteration, and after different times of alteration: (b) 2 weeks; (c) 4 weeks; (d) 6 weeks; (e) 10 weeks. The potential scan was initiated in negative direction, at 20 mV s^{-1}.

From the previous description, the pyrrhotite voltammetric behavior is strongly affected by the alteration process; in fact, evidence shows that the mechanism of alteration follows a mechanism similar to that of the mineral electrochemical oxidation. However, it is difficult to establish which stage of the electrochemical oxidation mechanism is being favored according to the time of alteration. This is because the electrochemical oxidation process of the altered samples does not exhibit specific changes for each superficial layer chemically formed on pyrrhotite. For the purpose of establishing which of the electrochemical and chemically formed products has the more significant effect in the reactivity of the pyrrhotite, an analysis of the different superficial species formed during the alteration process was carried out.

3.5. Species formed on pyrrhotite surface during the alteration process

According to prior electrochemical results, if it is assumed that the first stage of the pyrrhotite electrochemical oxidation mechanism is associated with the formation of a metal-deficient sulfide, then the voltammetric response obtained for the samples after 2 weeks of alteration must correspond mainly to the voltammetric response of the metal-deficient sulfide formed during this alteration period. On the other hand, the decrease in the global slope of the oxidation process may be related to the formation of a layer that limits the mass transport from the bulk solution to the reactive surface. This layer must be a porous layer of Fe precipitates, formed from the Fe dissolved from the first stages of alteration, such

as indicated by the maximum in the Fe concentration around 4 weeks of alteration (Fig. 2). Finally, the marked difference between voltammetric responses for pyrrhotite with alteration times greater than 4 weeks, suggests that important changes in the pyrrhotite surface state must have occurred at this alteration stage. These changes must have been caused by the formation of surface layers additional to the Fe oxy-hydroxide and metal-deficient sulfide layers. This new surface state must be related to the formation of elemental S provoked by the Fe release from the structure of metal-deficient sulfide according to reaction (6).

The presence of these 3 layers on the pyrrhotite surface was also demonstrated by SEM (Fig. 5). This figure shows images of pyrrhotite particles after 2, 4 and 10 weeks of alteration. After 2 weeks of alteration (Fig. 5(a)), the surface of the pyrrhotite shows a lamellar structure zone (point 1, Fig. 5(a)) and a surface layer covering this zone (point 2, Fig. 5(a)). The EDS microanalysis of these points revealed that the lamellar zone shows a decrease in Fe concentration against pyrrhotite bulk (Po), and that the most superficial layer (point 2) corresponds to a Fe–O rich compound. For samples after 4 week and longer alteration periods, the thickness of these 2 layers increases and a third layer (botroidal aspect zone) appears between them (point 3, Fig. 5(b) and (c)). The EDS microanalyses of this zone revealed that this is a S rich layer.

In order to analyze the effect of these oxidation products on the electrochemical behavior of the sample, voltammetric studies were performed on the 10 weeks alteration sample. The oxidized species were removed through selective leaching procedures. Hence, the Fe oxide layer was removed using a mixed solution of oxalic acid and ammonium oxalate, which is selective for Fe oxy-hydroxide species (Bousserrhine, 1995). The S layer

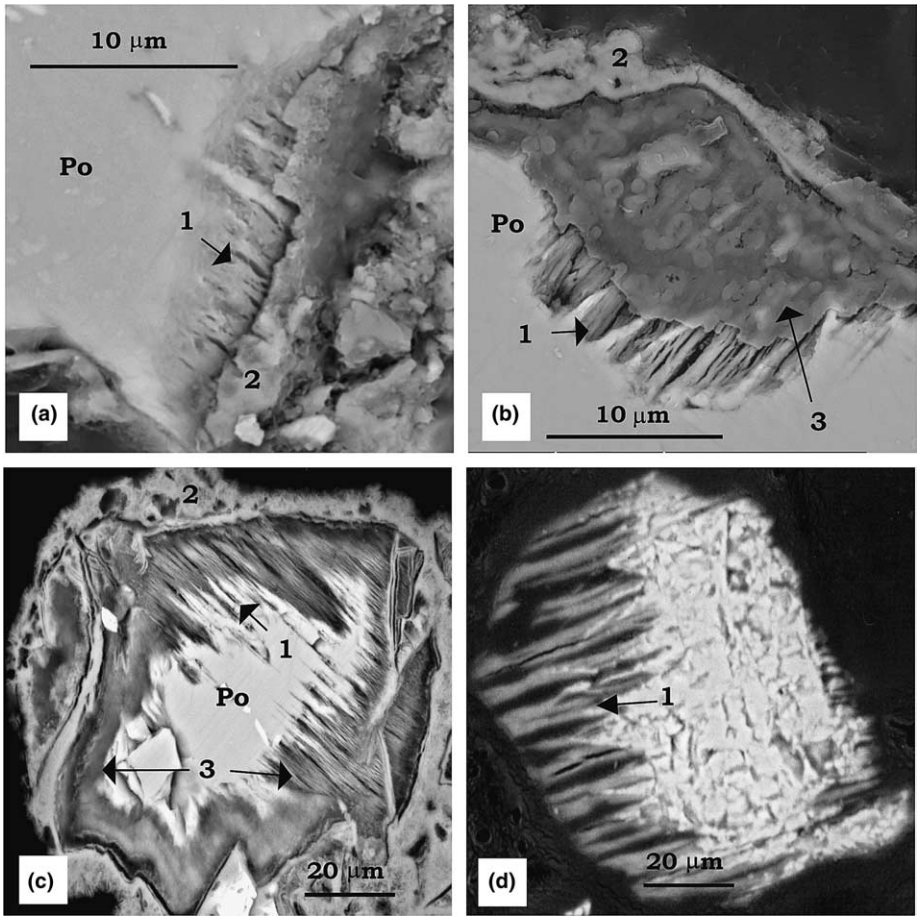

Fig. 5. SEM images of pyrrhotite particles after different times of alteration: (a) 2 weeks, (b) 4 weeks and (c) 10 weeks and (d) washed sample after 10 weeks of alteration. Po, pyrrhotite. The numbers on the images indicate: (1) lamellar structures with Fe content lower than that of pyrrhotite; (2) Fe- and O-rich phase and (3) phase of mostly S composition. The images were obtained from mineral particle polished sections.

was washed out using carbon disulfide. The effective elimination of the Fe-rich and S-rich layers was proved by X-ray diffraction (Fig. 6) and SEM observations (Fig. 5(d)). The X-ray diffraction results obtained for the washed samples indicate that the remaining material had a structure similar to a Fe sulfide with a pyrrhotite structure. The SEM observation shows that the washed pyrrhotite surface exhibits a lamellar structure (Fig. 5(d)).

The comparison between the voltammogram obtained for the washed and unwashed 10 weeks alteration samples of pyrrhotite is shown in Fig. 7. From this comparison it can be seen that when the Fe oxide layer has been removed, the electrochemical oxidation processes are similar to the unwashed sample and only the current associated with this process undergoes a decrease (Fig. 7), this fact confirms that the layer of Fe oxy-hydroxides represents only a diffusion barrier during the electrochemical oxidation. When the S layer was also eliminated the sample exhibited important changes in its voltammetric behavior (Fig. 7). Once the S and Fe oxy-hydroxide layers have been removed, it would be supposed that the Fe-deficient sulfide layer would be the only alteration product remaining on the pyrrhotite surface. It would be expected that the voltammetric response obtained for this sample would exhibit a similar behavior to that obtained for a sample with 1 or 2 weeks of alteration (the alteration time when Fe-deficient sulfide is presumably formed). Hence, the voltammetric responses obtained for the sample with 2 weeks of alteration and the washed sample show very similar behavior during the reverse scan (peaks R1, R3 and R4), but it is important to note that they differ in the anodic processes (peak O1). The differences in the ano-

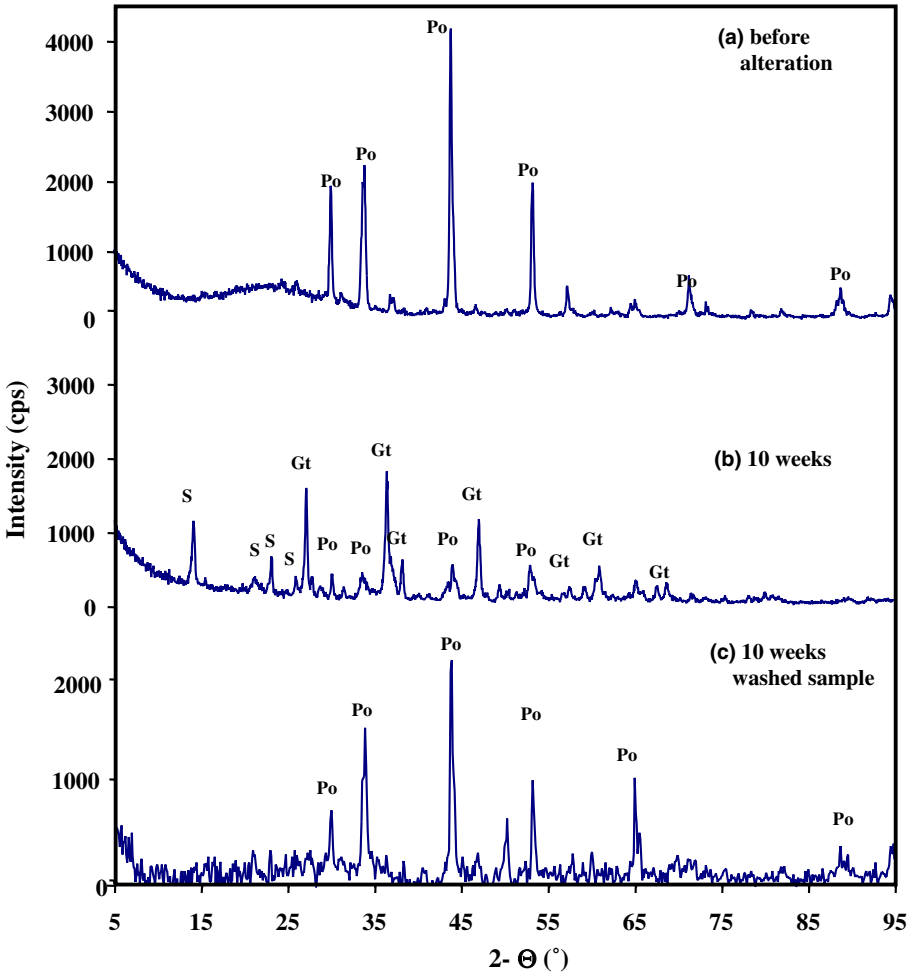

Fig. 6. X-ray diffractograms of pyrrhotite sample (a) before alteration (b) after 10 weeks of alteration and (c) after the Fe oxy-hydroxide and the S have been removed: Po, pyrrhotite; Gt, goethite; S, elemental sulfur.

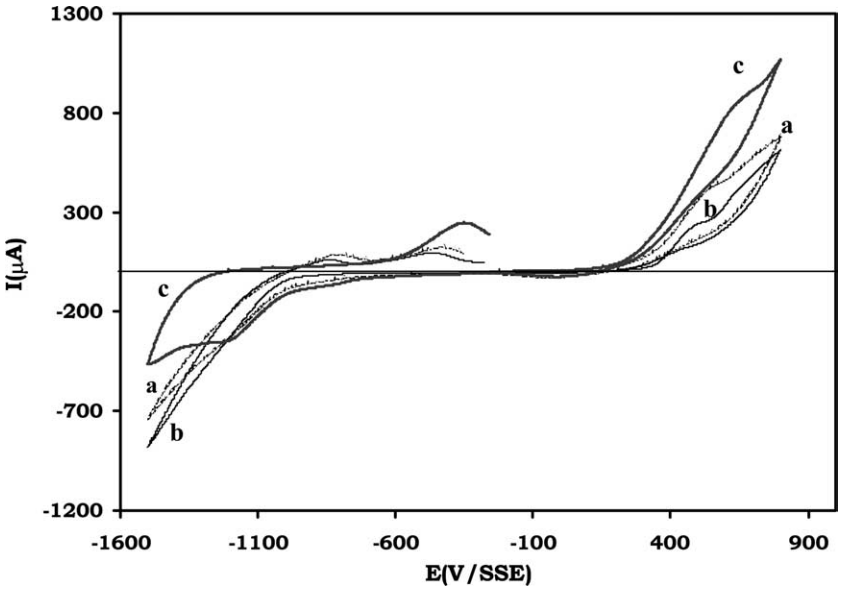

Fig. 7. Cyclic voltammetric response of CPE-pyrrhotite with 10 weeks of leaching before surface phase elimination (a), after eliminating the surface layer of Fe oxy-hydroxide (b) and after eliminating S and Fe oxy-hydroxide (c). The potential scan was initiated in positive direction, at 20 mV s^{-1}.

dic processes are due to the high specific area for the washed sample (Fig. 5(d)), which avoids the pasivation process of the surface, across the potential range analyzed.

3.6. Factors affecting pyrrhotite reactivity

Several authors have reported the high reactivity of pyrrhotite (Buckley and Woods, 1985a; Jambor, 1994;

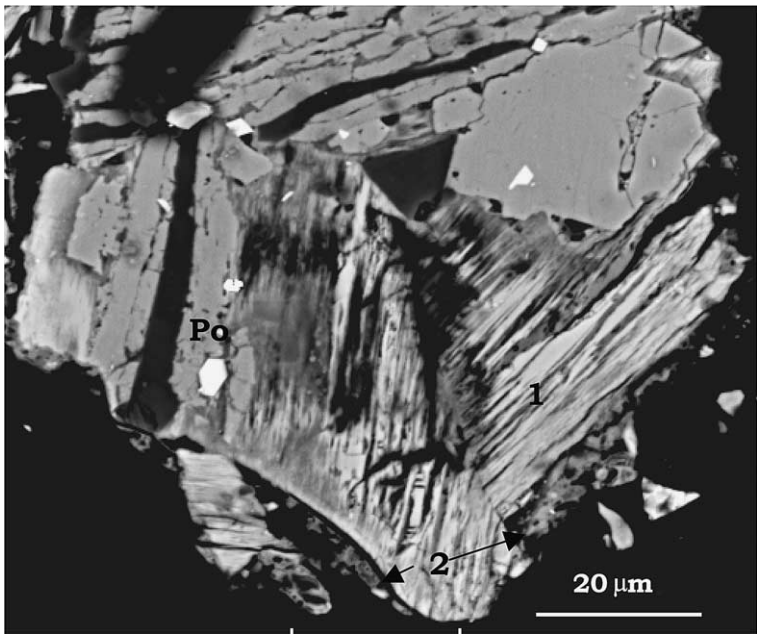

Fig. 8. SEM image of pyrrhotite particle from historic impoundment (sample was weathered in humidity cells). Po, pyrrhotite. The numbers indicate: (1) lamellar structures with Fe content lower than that of pyrrhotite; (2) Fe- and O-rich phase. The images were obtained from mineral particle polished sections.

Janzen et al., 2000). In the present work, this reactivity was shown by fast Fe dissolution in the first stages of the alteration process (Fig. 2(b)). However, after subjecting pyrrhotite to the alteration process over 3 weeks, the concentration of dissolved Fe in the leachate decreased significantly. This decrease was due to the formation of Fe precipitates (i.e., FeOOH) on the pyrrhotite surface. In this work the presence of these Fe precipitates resulting from pyrrhotite oxidation is proposed on the basis of the electrochemical study and corroborated by the SEM-EDS study. With the information obtained through the electrochemical study it was also possible to establish that in addition to the FeOOH precipitates, metal-deficient sulfide and elemental S layers are formed on the surface of the mineral during the alteration of pyrrhotite under simulated weathering conditions. The formation of similar layers on the mineral surface has been observed for pyrrhotite in mining residues showing weathering alteration obtained in the field, and in humidity cells (Fig. 8). This fact could be considered as a validation of the results here obtained.

With surface characterization through voltammetric analysis of the sample with and without superficial oxidation products, it was observed that the S layer actually governs voltammetric behavior of pyrrhotite after more than 4 weeks of alteration. These results suggest that the formation of the passivating S layer affects the reactivity of pyrrhotite more significantly than the diffusion barrier of the FeOOH layer. It is worth noting that the coupled effect of these layers must represent an important effect on the reactivity of the pyrrotite sample at advanced alteration stages, such as is suggested by the increasing pH and the low metal dissolution observed after 10 weeks of leaching (Fig. 2).

4. Conclusions

Cyclic voltammetry using C-paste electrodes represents an useful tool in the analysis of the reactivity of pyrrhotite under weathering conditions. The results of an initial voltammetric analysis of pyrrhotite before alteration was used as a reference for the characterization of the evolution of pyrrhotite reactivity during, laboratory simulated conditions of environmental alteration.

The systematic study of cyclic voltammetry of leached mineral samples in a mini-cell device, combined with chemical analysis and conventional techniques of mineralogical characterization (XRD and SEM-EDS), allowed the study of the evolution of pyrrhotite reactivity during the alteration process. Because of this study it was possible to establish that pyrrhotite alteration under environmental conditions follows a mechanism similar to that suggested by the voltammetric study. The results of this study suggest that pyrrhotite oxidation involves the formation of 3 surface layers: (1) in immediate contact with pyrrhotite corresponding to a metal-deficient sulfide; (2) an intermediate layer corresponding to elemental S, and; (3) the most external layer, consisting of precipitates of Fe oxy-hydroxides, like goethite. Similar results have been observed for pyrrhotite occurring in weathered mining sites and pyrrhotite under simulated weathering conditions in humidity cell procedures.

The formation of surface layers of Fe oxy-hydroxides and elemental S during the alteration process of pyrrhotite seems to be the principal factor that affects the pyrrhotite reactivity. The effect of the appearance of these layers on the pyrrhotite reactivity could be difficult to show using conventional methodologies of ARD prediction. However, because of the advantages of the presented methodology to monitor the mineral surface state evolution, it could be used to determine how the surface state has evolved and thus the affect on the mineral reactivity. This fact is indicative of the potential application and contribution of this methodology as a supporting tool in the study and prediction of ARD generated by alteration of sulfide mining residues with high pyrrhotite content.

Acknowledgments

This work was carried out thanks to the financial aid of the Mexican National Council of Science and Technology (CONACyT) Grant 25715B. Roel Cruz is grateful to CONACyT for the fellowship given for his doctoral studies. Thanks to Blanca Méndez who supported the realization of alteration tests. The authors are also grateful to the Research and Technological Development Center of Servicios Industriales Peñoles (CIDT-SIPSA, Monterrey, NL, Mexico) for the pyrrhotite sample and the chemical analyses.

References

American Society for Testing and Materials, 1996. ASTM Designation: D5744-96–Standard Test Method for Accelerated Weathering of Solid Materials Using Modified Humidity Cell, ASTM, West Conshocken, PA.

Bousserrhine, N., 1995. Étude de parametres de la reduction bacterienne du fer et application a la deferrification de mineraux industriels. Ph.D. Thesis, Univ. Henri-Poincaré Nancy.

Buckley, A.N., Woods, R., 1985a. X-ray photoelectron spectroscopy of oxidized pyrrhotite surfaces, I. Exposure to air. Appl. Surf. Sci. 22 (23), 280–287.

Buckley, A.N., Woods, R., 1985b. X-ray photoelectron spectroscopy of oxidized pyrrhotite surfaces, II. Exposure to aqueous solutions. Appl. Surf. Sci. 20, 472–480.

Buckley, A.N., Hamilton, I.C., Woods, R., 1988. Studies of the surface oxidation of pyrite and pyrrhotite using X-ray

photoelectron and linear potential sweep voltammetry. In: Woods, R., Richardson, P. (Eds.), International Symposium of Electrochemical of Metals and Minerals Processing II, vol. 21. The Electrochemical Society, pp. 234–246.

Cruz, R., 2000. Caracterización Electroquímica del Estado Superficial de Sulfuros Minerales de Hierro: Factores que afectan la biooxidación de minerales sulfurosos y la reactividad de pirita y pirrotita en la generación de drenaje ácido de roca. Ph.D. Thesis. Universidad Autónoma Metropolitana, México.

Cruz, R., Bertrand, V., Monroy, M., Gonzalez, I., 2001. Effect of sulfide impurities on the reactivity of pyrite and pyritic concentrates: a multi-tool approach. Appl. Geochem. 16, 803–819.

Doyle, F.M., Mirza, A.H., 1990. Understanding the mechanism and kinetics of acid and heavy metals release from pyritic wastes. In: Doyle, F.M. (Ed.), Proceedings of the Western Regional Symposium on Mining and Mineral Processing Wastes. AIME Pub. (Chapter 6).

Evangelou, V.P., 1995. Pyrite Oxidation and Its Control: Solution Chemistry Surface Chemistry, Acid Mine Drainage. CRC Press, Florida.

Hamilton, I.C., Woods, R., 1981. An investigation of surface oxidation of pyrite and pyrrhotite by linear potential sweep voltammetry. J. Electroanal. Chem. 118, 327–343.

Hojo, M., Peters, E., 1981. Direct electrorefining of chalcocite. J. Electroanal. Chem. 118, 345–364.

Jambor, J.L., 1994. Mineralogy sulfide-rich tailing and their oxidation products. In: Jambor, J.L., Blowes, W. (Eds.), Short Course Handbook on Environmental Geochemistry of Sulfide Mine-Wastes. Mineralogical Association of Canada.

Janzen, M.P., Nicholson, R.V., Scharer, J.M., 2000. Pyrrhotite reaction kinetics: reaction rates for oxidation by oxygen, ferric iron, and for nonoxidative dissolution. Geochim. Cosmochim. Acta 64, 1511–1522.

Laajalehto, K., Kartio, I., Suoninen, E., 1997. XPS and SR-XPS techniques applied to sulfide mineral surfaces. Int. J. Miner. Process. 51, 163–170.

Lazaro, I., Martinez, N., Arce, E., Rodrígez, I., González, I., 1995. The use of carbon pate electrodes with non-conducting binder for the study of minerals: Chalcopyrite. Hydrometallurgy 38, 275–285.

Lowson, R.T., 1982. Aqueous oxidation of pyrite by molecular oxygen. Chem. Rev. 82 (5), 462–493.

Mikhlin, Y.K., 2000. Reactivity of pyrrhotite surfaces: an electrochemistry study. Phys. Chem. Chem. Phys. 2, 5672–5677.

Mikhlin, Y.K., Kuklinskiy, A.V., Pavlenko, N.I., 2002. Spectroscopic and XRD studies of the air degradation of acid-reacted pyrrhotites. Geochim. Cosmochim. Acta 66 (23), 4057–4067.

Morin, K.A., Hutt, N.M., 1997. Environmental Geochemistry of Minesite Drainage: Practical and Case Studies. MDAG Publising, Vancouver.

Nesbitt, H.W., Muir, I.J., 1994. X-ray photoelectron spectroscopic study of a pristine pyrite surface reacted with water vapor and air. Geochim. Cosmochim. Acta 58, 4667–4679.

Nicholson, R.V., Gillham, R.W., Reardon, E.J., 1990. Pyrite oxidation in carbonated-buffered solution: 2. Rate by oxide coatings. Geochim. Cosmochim. Acta 54, 395–402.

Nicol, M.J., Scott, P.D., 1979. The kinetics and mechanisms of the non-oxidative dissolution of some iron sulphides in aqueous acidic solutions. J. S. Afr. Inst. Min. Metall. 79, 298–305.

Sand, W., Gehrke, T., Jorza, P.G., Schippers, A., 1999. Direct-versus indirect bioleaching. Process Metall. (Biohydrometallurgy and the environment towards the mining of the 21st Century, Part A), 27–49.

Sasaki, K., 1994. Effect of grinding on the rate of oxidation of pyrite by oxygen in acid solutions. Geochim. Cosmochim. Acta 58 (21), 4649–4655.

Sasaki, K., Tsunekawa, M., Ohtsuka, T., Konno, H., 1995. Confirmation of a sulfur-rich layer on pyrite after oxidative dissolution by Fe(III) ions around pH 2. Geochim. Cosmochim. Acta 59 (15), 3155–3158.

Shuey, R.T., 1975. Semiconducting Ore Minerals. Developments in Economic Geology Series 4. Elsevier Science Publishing, Amsterdam.

Steger, H.F., 1982. Oxidation of sulfide minerals. VII. Effect of temperature and relative humidity on the oxidation of pyrrhotite. Chem. Geol. 35, 281–295.

Thomas, J.E., Skinner, W.M., Smart, R., 2001. A mechanism to explain sudden changes in rates and products for pyrrhotite dissolution in acid solution. Geochim. Cosmochim. Acta 65, 1–12.